

Article

Use of Rotary Ultrasonic Plastic Welding as a Continuous Interconnection Technology for Large-Area e-Textiles

Christian Dils ^{1,*} , Sebastian Hohner ¹ and Martin Schneider-Ramelow ²¹ Fraunhofer IZM (Institute for Reliability and Microintegration), 13355 Berlin, Germany² Microperipheric Center, Technical University Berlin, 10623 Berlin, Germany

* Correspondence: christian.dils@izm.fraunhofer.de; Tel.: +49-30-46403-208

Abstract: For textile-based electronic systems with multiple contacts distributed over a large area, it is very complex to create reliable electrical and mechanical interconnections. In this work, we report for the first time on the use of rotating ultrasonic polymer welding for the continuous integration and interconnection of highly conductive ribbons with textile-integrated conductive tracks. For this purpose, the conductive ribbons are prelaminated on the bottom side with a thermoplastic film, which serves as an adhesion agent to the textile carrier, and another thermoplastic film is laminated on the top side, which serves as an electrical insulation layer. Experimental tests are used to investigate the optimum welding process parameters for each material combination. The interconnects are initially electrically measured and then tested by thermal cycling, moisture aging, buckling and washing tests, followed by electrical and optical analyses. The interconnects obtained are very low ohmic across the materials tested, with resulting contact resistances between 1 and 5 mOhm. Material-dependent results were observed in the reliability tests, with climatic and mechanical tests performing better than the wash tests for all materials. In addition, the development of a heated functional prototype demonstrates a first industrial application.

Keywords: electronic textiles (e-textiles); interconnection technology; ultrasonic welding



Citation: Dils, C.; Hohner, S.; Schneider-Ramelow, M. Use of Rotary Ultrasonic Plastic Welding as a Continuous Interconnection Technology for Large-Area e-Textiles. *Textiles* **2023**, *3*, 66–87. <https://doi.org/10.3390/textiles3010006>

Academic Editor: Laurent Dufossé

Received: 22 December 2022

Revised: 12 January 2023

Accepted: 25 January 2023

Published: 28 January 2023



Copyright: © 2023 by the authors. Licensee MDPI, Basel, Switzerland. This article is an open access article distributed under the terms and conditions of the Creative Commons Attribution (CC BY) license (<https://creativecommons.org/licenses/by/4.0/>).

1. Introduction

Textiles have gained ubiquitous importance due to their scalability in manufacturing and numerous beneficial mechanical and protective properties. The first electrically heatable textiles and patents have been known since 1910 [1]. However, intensive research into the integration of electronics in textiles has only been carried out since the late 1990s [2] fueled by the progressive miniaturization of electronics and new material developments in combination with the megatrends of pervasive computing and the internet of things. Jumping to today, a large business growth for electronic textiles (e-textiles) is predicted within the next decade [3], whereby the potential application areas are constantly expanding [4] and are not limited by geometric sizes. Wicaksono et al. predict that the scale of future e-textiles will range from microns to kilometers [5]. Today, e-textiles are already used for flexible heaters [6], wearable antennas [7] or large-area illumination [8], and also for monitoring bio-signals [9], vital data [10] and in situ structural health monitoring of composite materials [11]. Yet, there are still challenges in the production of large-area e-textiles that stand in the way of further market penetration. These include, in particular, textile-compatible, scalable integration and interconnection technologies [12], process automation for cost reduction [13] and also improved washability [14] and sustainability [15].

Since textiles and electronics differ greatly in their material properties and dimensions, standard processes from electronics manufacturing cannot be readily transferred to textiles. For example, although some metallic textile conductors can be soldered even with low contact resistances, these brittle connections do not provide reliable mechanical contact. In recent years, numerous more textile-compatible interconnection processes have been

developed, but most of them focus on contacting rigid electronic components or assemblies by means of interposers on a flexible textile substrate [16]. New e-textile production developments include, for example, the ZSK RACER 1W embroidery machine with an integrated circuit board laying unit, which can be used to realize automated embroidered contacts for a rigid interposer with conductive yarns [17]. Another solution was presented by Fraunhofer IZM, where a large-format bonder was developed [18], enabling the electrical and mechanical integration of multi-I/O modules on a textile substrate of up to $1\text{ m} \times 1\text{ m}$ by non-conductive adhesive bonding [19].

While science and industry have shown that it is possible to realize scalable and reliable textile integration of various types of hard components through novel joining technologies, purely fiber- or yarn-based interconnects still represent a major challenge for the development of textile-based electronic systems. In textile-heavy e-textiles, the electronic function is essentially provided by the textile, which provides more comfort and reliability than integrated systems made of hard and soft materials. Applications include the realization of conductive tracks and sensors made of conductive yarns, the integration of RFID chips directly into the yarn [20], or the development of fiber-based electronic, optoelectronic, energy-collecting, energy-storing and sensory devices that can be integrated into multifunctional e-textile systems [21].

Dhawan et al. presented the first results on studies of fiber-to-fiber contacts [22]. They integrated copper yarns orthogonally into a plain weave and modeled and experimentally determined the contact resistances at the crossing points of the conductive yarns. They found a strong influence of an acting force, which can also occur due to the movement of the textile, on the value of the contact resistance and recommended a further joining process to realize a mechanically stable interconnection. Using resistance welding (RW), they were able to achieve a crossover point interconnect resistance of 31 mOhm. Zhang, for example, uses the pressure-dependent contact resistance of multiple yarn-to-yarn contacts to develop a knitted strain sensor [23]. Suchý et al. describe that embroidered hybrid conductive yarns contacted by RW achieve a contact resistance of 10 mOhm [24]. The contacts showed stable values after dry heat, temperature shock and bending tests, but failed after washing tests. To optimize the washability, they propose additional encapsulation of the brittle contacts. For this purpose, thermoplastic films were subsequently applied to the contacts by ultrasonic welding or by lamination. While the ultrasonic welding damaged the brittle contacts to the point of failure, the laminated-over contacts were found to reliably withstand the washing tests [25]. Locher presents a different approach, in which a woven fabric was developed with intersecting copper wires insulated from each other by polyester threads [26]. Individual junctions, called textile vias, are first exposed by a laser ablation process. A drop of conductive adhesive is applied to the ablated area connecting the two crossing wires, and then epoxy resin is added as mechanical and electrical protection for the joint. The DC contact resistance obtained is 14.1 mOhm.

To reduce the very labor-intensive, multi-step process required to achieve a mechanically and electrically stable yarn-to-yarn contact, researchers have investigated ultrasonic plastic welding (UPW). UPW is a very efficient and ultra-fast joining process that is already established in the textile and packaging industries. Since many textiles have thermoplastic components, or thermoplastics can be easily added to an e-textile system in numerous forms, for example, as an electrical insulation layer or film-like structure, the otherwise necessary stripping, interconnection and encapsulation steps can be reduced to a single ultrasonic welding step. Slade and Winterhalter first described this approach for developing a selectively enabled wiring in textiles toolkit as follows: "This welding process melts the insulation around the wires and the polymer material (e.g., nylon or polyester) in the yarn, allowing the conductive cores of the wires to come into contact with each other. When the flow of ultrasonic energy into the weld site is stopped the polymer material surrounding the wires rapidly cools and hardens. As a result, the conductive cores of the wires remain locked in contact with each other, insulated from the environment. The result is a durable, easily achieved interconnection amongst selected conductors in an E-textile fabric, garment,

or textile article. By forming an ultrasonic weld at a defined point, conductive elements within the fabric can be made to form permanent connection with one another, for instance across a seam or between warp and weft yarns" [27]. The first experimental studies on ultrasonically welded contacts for e-textiles were only published in recent years. Thurner describes the UPW of electrically conductive adhesive nonwovens with silver-coated yarns, where low contact resistances of 10 mOhm were obtained [28]. It is also reported that the welded contacts can withstand high ampacity loads of 10 A and mechanical tests such as bending, flexing or torsion for 10,000 cycles without major resistance changes. Micus et al. investigated the UPW for contacting a knitted conductive textile with copper stranded wires, measuring a contact resistance of 1.95 Ohm [29]. After the washing tests, the contact resistances increased threefold, which the authors attributed mainly to the damage of the selected silver-coated yarns. Dils et al. report on electrical and mechanical contacting of rigid interposers with silver-metallized nonwovens using a thermoplastic film and UPW [30]. By adapting the contact structures and process parameters, they realized electrical contacts in the range < 20 mOhm, providing material-dependent results in reliability. Another study by Dils et al. investigated the interconnection of two embroidered hybrid conductive yarns at their crossing point [31]. In their study, by adapting the embroidered contact pad design and using an experimental setup, process parameters for different material combinations could be investigated. Simultaneous encapsulation of the contacts was achieved by using a TPU cover layer pre-placed over the crossing point. The average contact resistance of the samples was below 2.5 mOhm and showed no changes even after mechanical and environmental reliability tests.

In addition to the presented investigations using ultrasonic spot welding for yarn-to-yarn interconnects, there are also publications on the continuous ultrasonic plastic welding (CUPW) process for e-textiles but they only investigate the bonding of conductive materials on textile substrates. Atalay et al. use the CUPW process to integrate various conductive yarns into a waterproof polyester fabric as signal lines for e-textiles applications [32]. They examined the influence of the welding parameters on the conductivity and seam strength of the selected materials. Leśnikowski investigated the textile integration of nickel-coated polyester strips as a single or double layer using CUPW to fabricate transmission signal lines [33]. He reported that direct welding caused damage in the conductive tape or short circuits that did not occur when a double-sided textile outer layer was added. Furthermore, the samples made in this way allowed the construction of signal lines capable of transmitting DC and AC signals at frequencies up to several hundred MHz.

The aim of this work is to investigate and analyze the continuous interconnection of textile conductor materials by CUPW. To the best of our knowledge, this is the first study on the subject. Based on the results from the presented studies on spot interconnects of crossing embroidered hybrid conductive yarns as well as the literature review, we target the use of metal strand-based textile conductors, since damage to metal-coated yarns and fabrics has often been reported. Several additional materials are investigated as adhesion agents and simultaneous electrical and mechanical insulation of the contacts, for example thermoplastic films without conductive particles, in order to consider requirements for resource efficiency and reparability. For large-area textile-based electronic systems, we focus on integrating embroidered conductors into the textile substrate and welding a conductive ribbon orthogonal to them, so that the multiple conductors can make electrical and mechanical contact with each other.

2. Materials and Methods

2.1. Welding Tools

The welding process was carried out on an 8312 flatbed ultrasonic machine from PFAFF Industriesysteme und Maschinen GmbH, which is equipped with a 10 mm wide steel sonotrode wheel. The ultrasonic generator has a working frequency of 35 kHz and a maximum power of 800 W. On the machine, a gap dimension of 0–2 mm with a fine adjustment of 1/50 mm can be set. The parameters welding speed (0.5–20.0 m/min),

welding force (0–400 N) and amplitude (from 18 μm to 34 μm for the sonotrode used (or 50–100%)) can also be adjusted. A knurled steel wheel with a width of 10 mm (PFAFF article number 95-256 126-05) was used as the anvil, which achieved the best welding results in preliminary tests. A pyramid wheel also showed suitability for welding but achieved inferior electrical results compared with the knurled wheel and produced wavy structures in the welded specimens. The smooth, zigzag or circular shaped anvil wheels did not produce repeatable mechanical and electrical connections in different test materials. Figure 1a shows a detailed view of the topography of the knurled wheel, and Figure 1b shows the welding of a conductive ribbon onto a conductive knit with the ultrasonic machine.

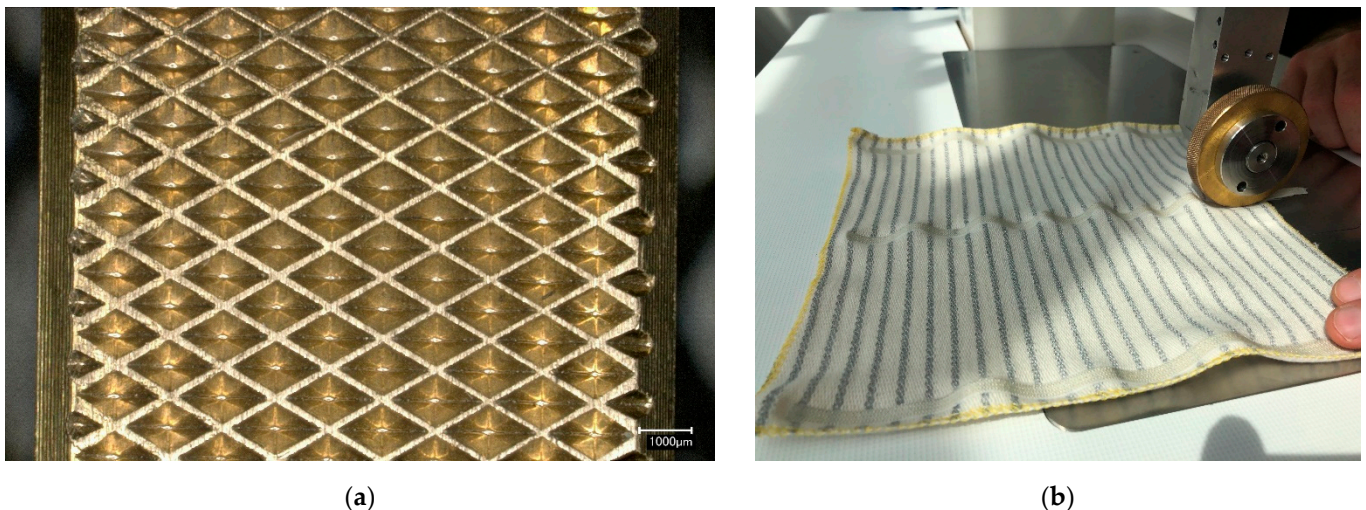


Figure 1. Ultrasonic welding tools: (a) detailed image of the surface structure of the knurled wheel; (b) anvil wheel of the Pfaff 8312 welding machine and welded specimen.

2.2. Substrate Materials

Elastic knitted fabrics were more difficult to process than non-elastic woven textiles and shrank during welding. Even the use of embroidery hoops to mechanically fix the elastic textiles did not lead to any improvements. Therefore, woven substrates were used for the trials in this study. Cotton is particularly suitable as a textile substrate material, as textiles made of polymers can melt during ultrasonic welding, which could lead to an undesired stiffening of the welding area. Therefore, a 100% plain weave cotton fabric with a weight per unit area of 190 g/m² was selected as the substrate.

Electrically conductive yarns were integrated into the textile substrate, with heating, conductor tracks, or sensors as possible functions. In total, four commercially available conductive yarns from the supplier VÚB a.s. and its Clevertex brand were selected for testing. All the yarn variants are characterized by the fact that they consist of a twisted yarn of textile polymer fibers and metal strands and are, therefore, referred to as hybrid conductive yarns. The hybrid conductive yarns are marketed as suitable for embroidery, knitting and weaving. Table 1 gives an overview of the four selected yarns, their composition and their properties according to the information provided by the manufacturer Clevertex.

One yarn type was available in two versions, without (Y08) and with thermoplastic insulation (Y09). Another yarn (Y12) was made of silver-metallized polymer threads in addition to silver-plated copper strands, which makes it more ductile overall. The last yarn selected (Y13) consisted of high-impedance stainless steel filaments.

2.3. Conductive Ribbon

While there are numerous weldable adhesive tapes, no electrically conductive ones are known. One exception was the conductive hotmelt adhesive non-woven e-Web 140 from the manufacturer imbut GmbH, which is available in rolls. However, the material cannot be processed with an ultrasonic welding device as it was observed in our tests

that using it damaged or destroyed both the conductive silver coating on the polymer fibers and the nonwoven material. We suspect that this is due to the impact of ultrasonic vibrations on the material. Due to this lack of suitable welding tape, we therefore, looked for conductive tapes or ribbons that are made weldable by means of a subsequent lamination with thermoplastic film.

Table 1. Properties of the selected conductive yarns as provided by the manufacturer Clevertex.

ID	Material Composition	Coating/Insulation	Linear Resistance (Ω/m)	Fineness (tex)	Diameter (mm)	Dry Strength (cN/tex)	Dry Elongation (%)
Y08	4 × PES threads, 8 × 0.03 mm Cu/Ag filaments	None	2.85	78	0.24	21.85	13.3
Y09	4 × PES threads, 8 × 0.03 mm Cu/Ag filaments	TPA	3.3	76	0.23	22.07	13.4
Y12	4 × 110 dtex/f24 SilverStat threads, 4 × 0.03 mm Cu/Ag filaments	None	6.6	84.9	0.29	16.11	53
Y13	4 × PES threads, 4 × 0.02 mm stainless steel filaments	None	560.5	37.6	0.22	46.91	15

PES: polyester; TPA: thermoplastic polyamide; Cu: copper; Ag: silver.

Four different types of conductive ribbons with a linear resistance significantly lower than 1 Ohm/m were selected for the experiments, which are presented in Table 2.

Table 2. Properties of the selected conductive ribbons.

ID	Manufacturer	Material Composition	Linear Resistance (Ω/m)	Width (mm)	Thickness (mm)
Elasta Vestil	ELASTA VESTIL a.s.	weft: 12/88 PET threads; warp: 34 × Y08 conductive yarns	0.14 (0.11 when embedded into TPU film)	8	0.5
High Flex 3981	Karl Grimm GmbH & Co. KG	33 × 1 PET threads (74 dtex) stranded with thin Cu/Ag foil	0.41 (0.42 when embedded into TPU film)	4	0.2
Amotape 3587	AMOHR Technische Textilien GmbH	PET threads, hotmelt yarns and 6 × Cu/Ag strands	0.07 (0.09 when embedded into TPU film)	9	0.54
Amotape 46050	AMOHR Technische Textilien GmbH	weft: 6 × Cu/Ag strands, hotmelt yarns and PET threads (84 dtex); warp: PET threads (140 dtex)	0.03	9	0.6

PET: polyethylene terephthalate; TPU: thermoplastic polyurethane.

Amotape 3587 was only used in the first trial, and Amotape 46050 is an optimized version and was only used in the following main trial. The main difference between the two versions is that in the second variant, the six conductive strands cross each other regularly to improve electrical characteristics and that it incorporates further hotmelt yarns which make an additional lamination of the TPU film unnecessary. Besides the electrical, material and size differences, the ribbons partially differ in the textile production. Except for the High Flex ribbon, which is braided, the other three ribbons are all woven. X-ray and cross-sectional images of the conductive ribbons are shown in Figures 2–6.

For sufficient bonding between textile-integrated conductor materials and the conductive ribbon, an additional adhesive was needed. In our study, we laminated an adhesive film to the conductive ribbon prior welding. Covestro Platilon 4201 AU polyurethane (ether) film in 100 μm thickness was used as an adhesive [34]. The material has proven itself in recent years as a suitable substrate material for soft and stretchable circuit boards [35–37] as well as an adhesion agent for e-textile non-conductive adhesive bonding technology [38]. Before the welding process, the TPU film was cut to a width of 10 mm and laminated to the

conductive ribbon on both sides using a Sefa HP45 2PS thermal press at 180 °C and 2 bar for 45 s. The laminate was afterwards cooled under pressure for a few minutes.

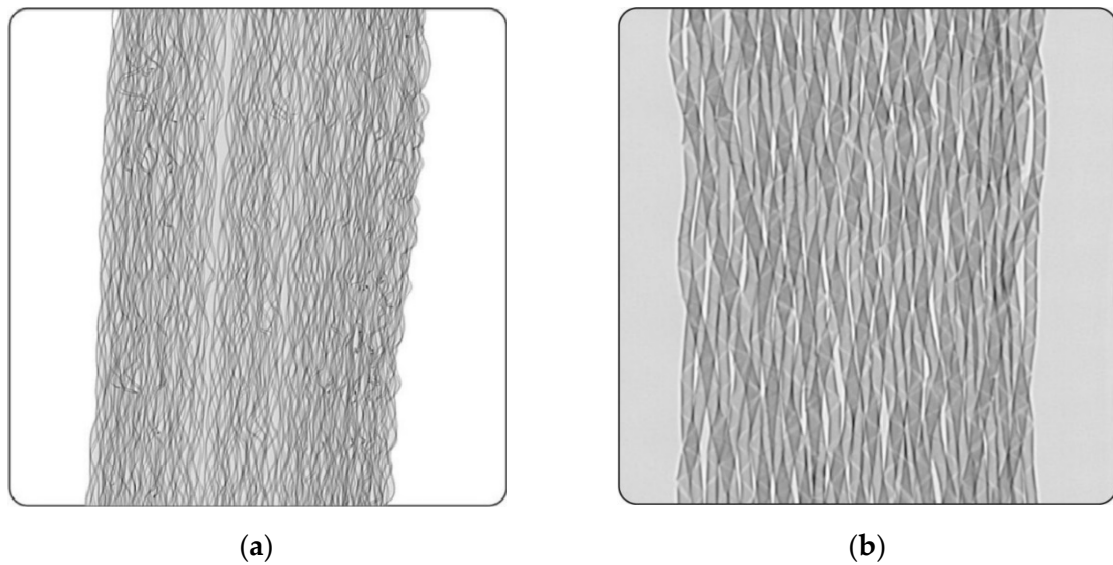


Figure 2. X-ray images of the selected conductive ribbons: (a) Elasta Vestil; and (b) High Flex 3981.

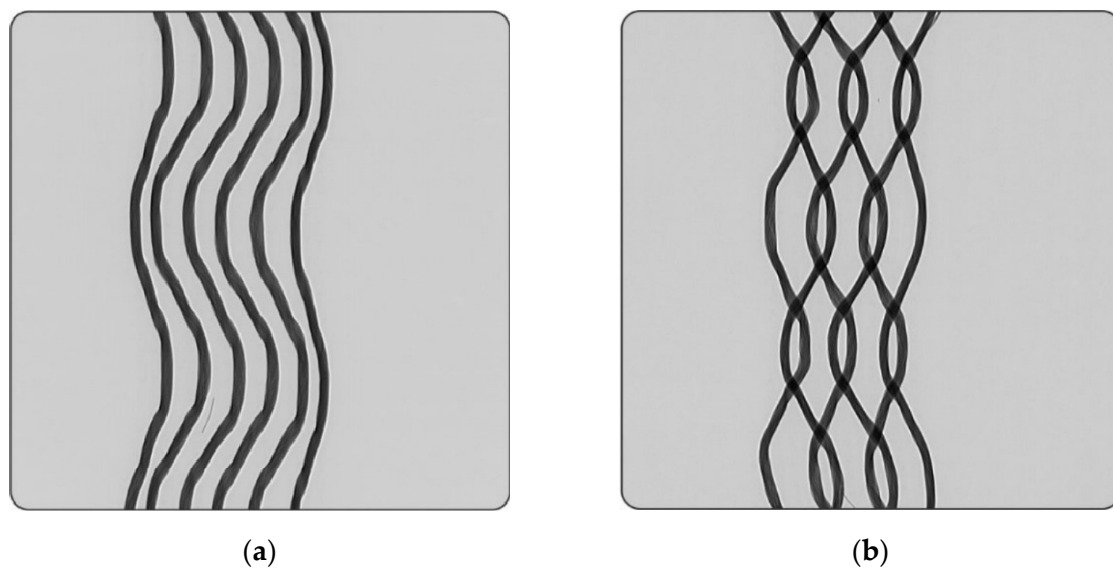


Figure 3. X-ray images of the selected conductive ribbons: (a) Amotape 3587; and (b) Amotape 46050.

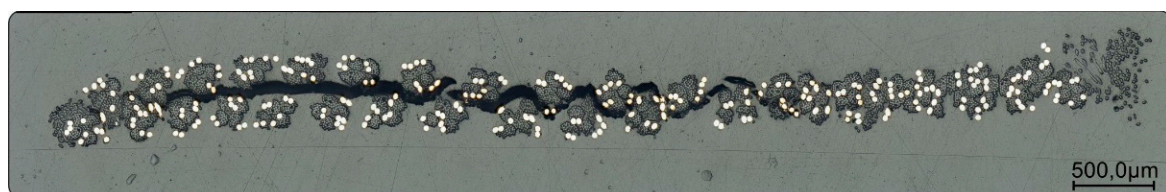


Figure 4. Cross-section image of the Elasta Vestil woven ribbon with 34 hybrid conductive yarns distributed over the entire area.



Figure 5. Cross-section image of the High Flex 3981 braided ribbon. In the zoom window, the individual yarns covered with thin silver-plated copper foil are shown for better visualization.



Figure 6. Cross-section image of the Amotape 3587 woven ribbon with six parallel-running bundles of silver-plated copper strands. The Amotape 46050 woven ribbon with six crossed bundles of silver-plated copper strands and additional hotmelt yarn is not displayed as the cross-sections of both Amotape versions are comparable.

2.4. Peel Strength of Welded Materials

To determine the adhesion strength, the optimum welding parameters were determined by the adhesion force between the conductive ribbons and the textile substrate. The conductive ribbons, partially pre-laminated with TPU, were ultrasonically welded onto the cotton substrate in a wide process window by modifying the welding parameters gap size, power, speed and force. Subsequently, a T-peel test was carried out according to IPC TM 650 standard [39], the peel forces were recorded, and the fracture pattern evaluated. Differing from the standard, peeling was not actuated at an 90° angle, but at an 180° angle due to the limp textile properties. The test parameters were a peeling speed of 50.8 mm/min and 3 repetitions per parameter and material combination, with a sample size of 10 mm × 80 mm. The peeling force F_p (N) was measured and standardized over the width a (mm) for better comparability. The resulting peeling force F_a (N/mm) was calculated according to Equation (1).

$$F_a = \frac{F_p}{a} \quad (1)$$

2.5. Shrinkage of Conductive Ribbons

To determine shrinkage effects due to thermal and mechanical impact during the welding process, the conductive ribbons were welded onto the cotton substrate using the best welding parameters determined from the peel tests. The samples were measured before and after welding and the shrinkage was calculated according to Equation (2). The results were then used in the adjustment of the sample lengths for the main tests.

$$S = \frac{L_0 - L}{L_0} \cdot 100 \quad (2)$$

Here, S is shrinkage in %, L_0 is initial length in mm and L is the resulting length in mm after welding.

2.6. Electrical Characterization of Materials and Interconnections

All the electrical measurements, both for the initial values of the conductive yarns and ribbons, as well as for the ultrasonically welded contact resistance R_c , were measured with the four-point method using a Keithley 2010 multimeter. This measurement method eliminates the influence of the resistance of embroidered conductor tracks, the resistance of the contact pins and the resistance of the connecting cables, so that only the linear resistance of the materials or the contact resistance of the welded interconnects were measured. For the initial material resistance measurements, the yarn and fabric procedures from the standard DIN EN 16812:2016-11 were applied [40].

In electrical characterization, the interconnections must be part of an electronic circuit and are considered as electrical resistances. The permissible value of the contact resistance depends on the electronic system and the desired application and is, therefore, not generally defined [41]. However, the lower the contact resistance, the better the signal quality and the lower the heat generation. A gradual increase in contact resistance, as determined by aging and durability tests, is also a good indicator of contact fatigue and can be caused by conductor dissolution, delamination of coatings, and cracks in coatings or conductors that can lead to electronic system failure over time [42,43].

In our study, a sudden loss of electrical connection, e.g., due to interruption of a previously stable conductor or a gradual increase in resistance above a threshold contact resistance R_{th} of 50 mOhm, was defined as a contact fault. This threshold value was based on the large contact area between the contact materials, which allows for low contact resistance, and on the initial measurements from the preliminary tests, where R_c values between 1 and 20 mOhm could be achieved, depending on the material. If the R_c value rises (steadily) to 50 mOhm, one can already assume a gradual degradation of the contact resistance.

2.7. Design of Test Pattern

A uniform test pattern was designed for easy evaluation and comparison of the effects of the welding process parameters and materials on the contact resistance of the welded joints. The test pattern was developed for the electrical four-point measurement and is shown in Figure 7a. The hybrid conductive yarns were first embroidered onto the cotton substrate to obtain the required 2D pattern, with the ends being designed as a measurement pad for easy electrical measurements. Then, the contact ribbons were linearly and continuously welded over the embroidered yarns, with the electrical interconnection being made at the point of intersection between the two contact partners (see Figure 7b).

2.8. Proposed Interconnection Process

The novel interconnection process for e-textiles is based on CUPW and works analogously to the welding of an adhesive seam tape onto textiles. Here, instead of joining two textile parts together, textile-integrated conductor materials are mechanically and electrically joined with a conductive ribbon or tape. The proposed interconnection process is shown schematically in Figure 8a,b. Friction welding generated by ultrasonic vibrations leads to strong molecular movements in the material interface layers, thereby generating heat in the joining zone and causing a reduction in the viscosity of the thermoplastic materials, resulting in local softening of the polymers. Due to the simultaneous application of force F , the conductor materials are pressed through the softened polymers and touch, creating an electrical contact. The material is then transported out of the welding zone by the wheel at a defined speed v and solidified again. Since the ultrasonic welding process is very fast, runs at room temperature, and does not require additional additives, such as solder flux or conductive particles in the adhesive, it is very efficient and resource saving and, therefore, well suited for industrial production.

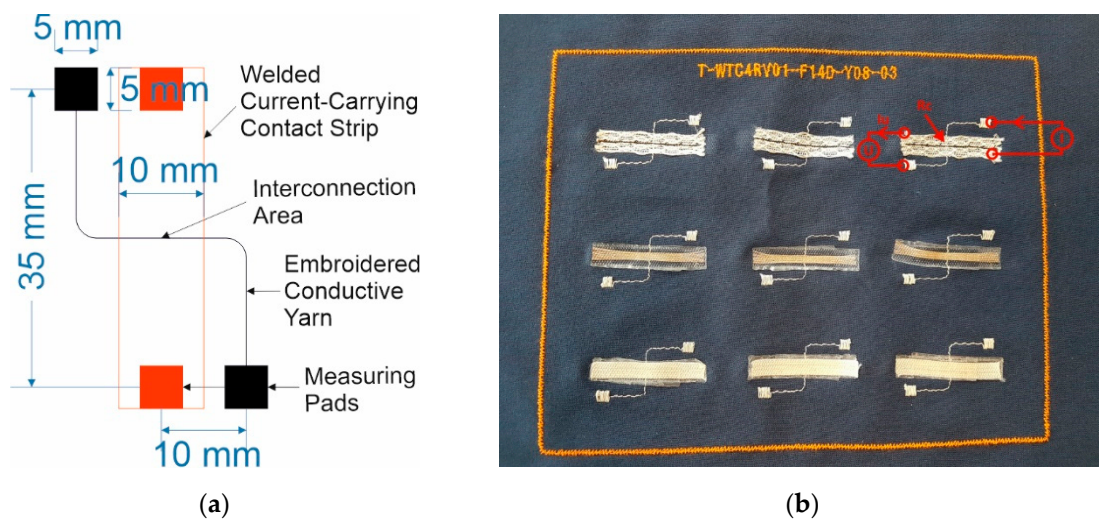


Figure 7. Test structure design: (a) pattern design; and (b) welded pattern sheet with one type of conductive yarn and three different types of conductive ribbons.

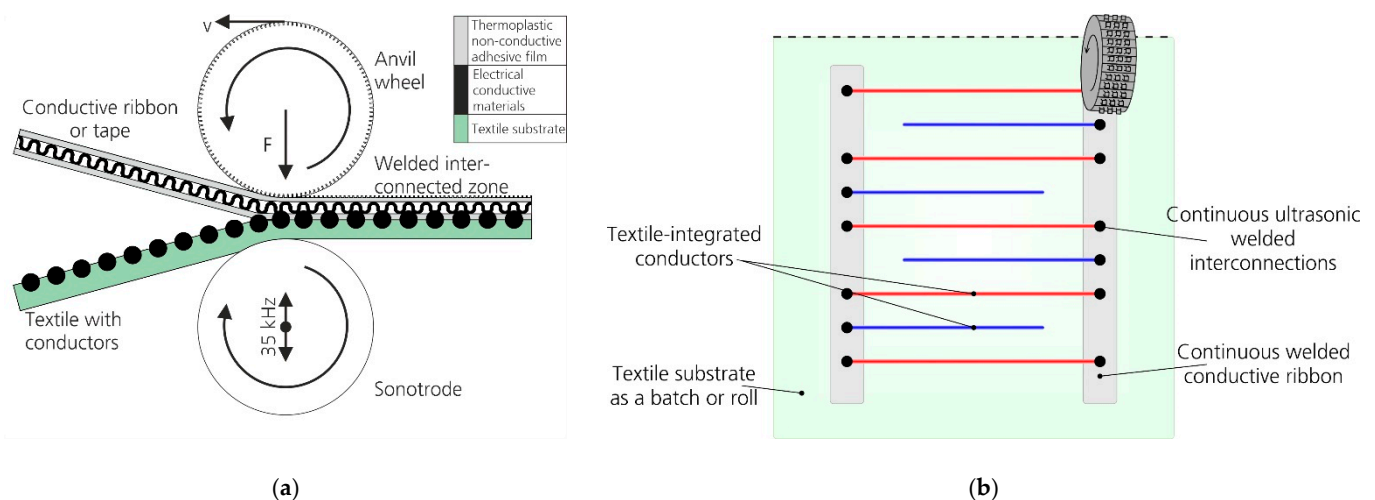


Figure 8. Schematic representation of the proposed continuous interconnection process using rotary ultrasonic welding: (a) the conductive ribbon is continuously welded to the textile substrate with the integrated conductors by means of an adhesive with contacts made at the crossing points; and (b) view of typical structures to be interconnected, here with conductors contacted on both sides (colored red) or interdigital structures contacted on one side (colored blue).

2.9. Reliability Tests of the Welded Interconnections

Reliability tests were applied to determine the lifetime and failure mechanisms of the welded interconnections. Due to the novelty of e-textiles, testing standards are not yet available or only for very limited specifications [44,45]. The challenge in the selection of reliability tests, therefore, also consisted of researching alternative existing standards and evaluating whether they are suitable for the materials, technologies and applications to be investigated. In addition, self-developed test methods were used if no existing standards were available.

Climatic tests were used to investigate thermal and moisture influence on the materials. The focus lay on both expansion and swelling of the polymers as well as the oxidation behavior of the metals, which can lead to delamination or impurity layers and thus to degradation of the welded interconnection. For reliability tests, the IEC 60068-2-14 and IEC 60068-2-1 (thermal cycling) as well as IEC 60068-2-78 (damp heat test) standards were applied, which are specified as general interconnection tests for electronic systems [46–48].

In the temperature-cycling test, the test specimens were held at 65 °C and −5 °C for 10 min each in ESPEC Corp’s TSA-102ES climatic shock chamber and cycled 500 times. In the humidity-heat test, the samples were maintained at a constant 40 °C and 93% RH for 240 h. This was done in the climate test chamber VC³ 7034 from Voetsch.

Due to the lack of standardized e-textile tests, a new method for mechanical reliability tests was necessary since conventional bending tests with limp textile materials lead to very large bending radii and can, therefore, only provide very limited information about mechanical reliability under more realistic buckling and folding loads. In our self-developed method for buckling load tests, the test specimen was fixed with rigid clamps, as shown in Figure 9a. Fixed clamps made of FR-4 PCB substrate material, were attached to both sides of the textile, and the distance between the upper and lower clamping elements determined the resulting bending angle. In the following experiments, a bending angle of 70° could be realized, as shown in Figure 9b. The tests were carried out on an INSTRON 5000 tensile testing machine at a buckling frequency of 1 Hz for 10,000 cycles per sample.

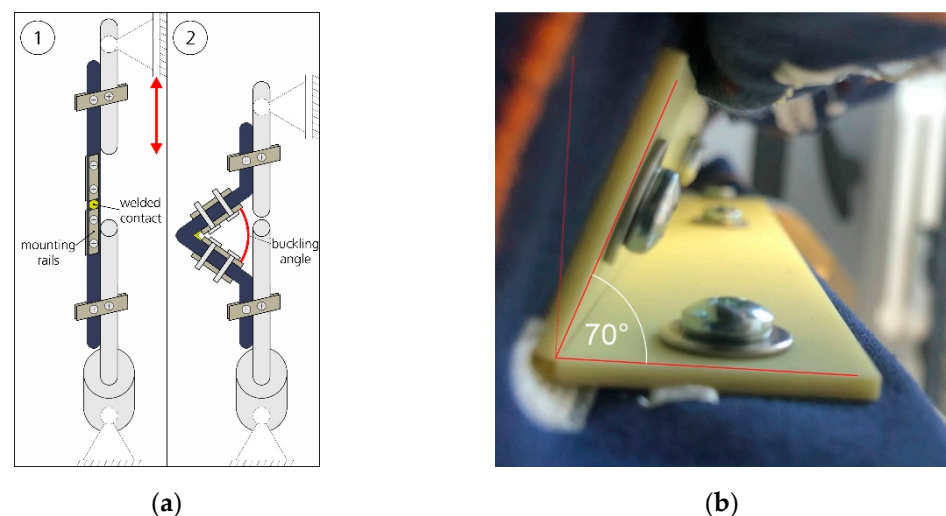


Figure 9. Test rig for mechanical buckling load of welded interconnections: (a) schematic representation of the buckling test; and (b) test sample in the buckling test with 70° buckling angle.

To date, there is no specific wash testing standard for e-textiles according to which standardized tests can be carried out. As a result, the test methods currently used by academia and industry are very different and thus not comparable. In addition, the existing textile washing standards are only suitable for e-textiles to a limited extent. In current research results, experts agree that gentle washing is necessary as a basis for a future standard for e-textiles [49,50]. A new test protocol based on gentle household washing and the ISO 6330 standard was published, tested for cleanability, and used for the wash tests in this study. The following washing conditions were taken from [51] (pp. 8–9):

- Washing program: main wash, intermediate spinning (500 rpm), two rinsing cycles, spinning (800 rpm); duration: 40 min; temperature: 30 °C; on-time: 40%; water volume: 12 l;
- load: additional PES base load items for a total weight of 2 kg including test samples;
- detergent: 30 g of ECE-2 standard powder detergent (adjusted amount according to used hard water);
- drying: air drying;
- number of cycles: 20.

3. Results

3.1. Determination of the Welding Process Parameters

For the peel tests, the conductive ribbons were welded onto the cotton fabric according to a test matrix with varying welding parameters for power P of 100–400 W, speed v of

0.2–1 m/min, force F of 100–400 N, and a material-adapted gap size s of 0.1–0.75 mm. The amplitude could not be changed in the manual power welding method with which method the tests were performed. The material-dependent highest measured peel forces are listed in Table 3 and compared with the required adhesive strengths of flexible electronic substrates.

Table 3. Highest determined peel forces from the welding test matrix for each conductive ribbon compared with required adhesion strength of conventional, flexible electronic substrates.

Material Combination	Standard	Peel Force F_H [N/mm]
Cotton/Elasta Vestil	None	0.7
Cotton/High Flex 3981	None	1.7
Cotton/Amotape 3587	None	0.4
Cotton/Amotape 46050	None	0.6
FR-4/Cu (35 μm)	DIN EN 60249-2-4	>1.4
PET/Cu (35 μm)	DIN EN 60249-2-8	>0.7
PI/Cu (35 μm)	DIN EN 60249-2-13	>0.8

PI: Polyimide.

Without additional TPU adhesives, the peel forces F_H for Elasta Vestil and High Flex 3981 would be only 0.0–0.1 N/mm and thus insufficient for integration and interconnection. The adhesion forces of the Amotape ribbons could be significantly higher with an additional adhesive, but this was not applied to save the additional material and lamination process step as this would be the most economically preferred option. Testing of the peel strength of standardized values for electronic substrates (where the adhesion strength between laminated copper foils and carrier material is determined) with the ultrasonically welded contact ribbons provided comparable results. In some cases, the specimens already met the required adhesion strength of conventional, flexible electronic substrates.

Adhesion fractures dominated the fracture pattern evaluation, except for the Amotape tapes not prelaminated with TPU, where mixed fractures were observed (See also Figure 10a,b).



Figure 10. Visual fracture determination of the samples after the peel tests: (a) mixed fracture for Amotape 3587; and (b) adhesion fracture for High Flex 3981 prelaminated with TPU.

From the results of the peel tests, it was confirmed that some optimum welding parameters are the same for all different samples: $P = 100$ W, $F = 100$ N, and $v = 0.2$ – 0.4 m/min. At higher powers, carbonization of the materials could be observed, which led to failures both visually and functionally. In addition, excessively high gap sizes and speeds do not allow melting and bonding of the contact partners. If the gap distances are too small, the materials are pressed too hard, which is noticeable as audible squeaking and can lead to damage to

the materials and welding tools. With the determined welding parameter windows, the next tests were carried out to measure the shrinkage of the conductive ribbons, with the results listed in Table 4.

Table 4. Determination of the shrinkage behavior of the welded conductive ribbons.

Value	Elasta Vestil	High Flex 3981	Amotape 3587
Initial length L_0 (mm)	39.5	39.4	38.7
Length after welding L (mm)	36.8	36.4	38.7
Shrinkage S (mm)	2.7	3	0
Shrinkage S (%)	6.8	7.6	0

The TPU-laminated conductive ribbons shrank between 6.8 and 7.6% due to the ultrasonic welding process. Therefore, in the following interconnection welding tests, the lengths of the Elasta Vestil and High Flex 3981 ribbons were adjusted.

3.2. Interconnection Welding Tests and Contact Resistances

Cotton substrates were embroidered with the four selected conductive hybrid yarns by the external partners VÚB a.s. and University of West Bohemia and provided for this study. The pre-determined welding parameters for each yarn are listed in Table 5. While power ($P = 100$ W) and force ($F = 100$ N) remained the same in the welding interconnection tests, the speed v and gap size s were varied depending on the different diameters of the yarns as well as the thickness of the ribbons.

Table 5. Process parameters for determining speed and gap size values for optimization of welded contact resistances.

Ribbon	Yarn	Speed v (m/min) for Parameter 1–3	Speed v (m/min) for Parameter 4–5	Gap Size s (mm) for Parameter 1	Gap Size s (mm) for Parameter 2	Gap Size s (mm) for Parameter 3	Gap Size s (mm) for Parameter 4	Gap Size s (mm) for Parameter 5
Elasta Vestil	Y08	0.4	0.4	0.2	0.3	0.4	0.6	0.8
	Y09	0.4	0.4	0.3	0.4	0.5	0.7	0.9
	Y12	0.4	0.4	0.35	0.45	0.55	0.75	0.95
	Y13	0.4	0.4	0.15	0.25	0.35	0.55	0.75
High Flex 3981	Y08	0.2	0.4	0.1	0.2	0.3	0.1	0.2
	Y09	0.2	0.4	0.2	0.3	0.4	0.2	0.3
	Y12	0.2	0.4	0.25	0.35	0.45	0.25	0.35
	Y13	0.2	0.4	0.05	0.15	0.25	0.05	0.15
Amotape 3587	Y08	0.2	0.4	0.1	0.2	0.3	0.1	0.2
	Y09	0.2	0.4	0.2	0.3	0.4	0.2	0.3
	Y12	0.2	0.4	0.25	0.35	0.45	0.25	0.35
	Y13	0.2	0.4	0.05	0.15	0.25	0.05	0.15

Figures 11–14 show the obtained and measured results on the welded contact resistances of the corresponding conductive ribbon/yarn combinations. The results are presented as box plots since with 10 or 11 individual tests per combination, sufficient values were available for a statistical evaluation. An auxiliary line at 50 mOhm is drawn to clearly indicate the target value for the contact resistance formulated in Section 2.6. The Y13 yarn variant developed for heating applications consists of only a very few stainless-steel filaments, and therefore, has a very high resistance, which is why the measured contact resistances here clearly exceed the 50 mOhm threshold value of R_c . The combination of Y13 and High Flex 3981 did not achieve an electrical contact in any test; therefore, no diagram is provided. For a better overview of the results obtained, the Y-axis in several diagrams was scaled differently and drawn in two colors. A blue ordinate axis indicates a contact resistance in the lower ohm range, a red one in the higher ohm range and the sign “X” stands for an electrical fault in all diagrams.

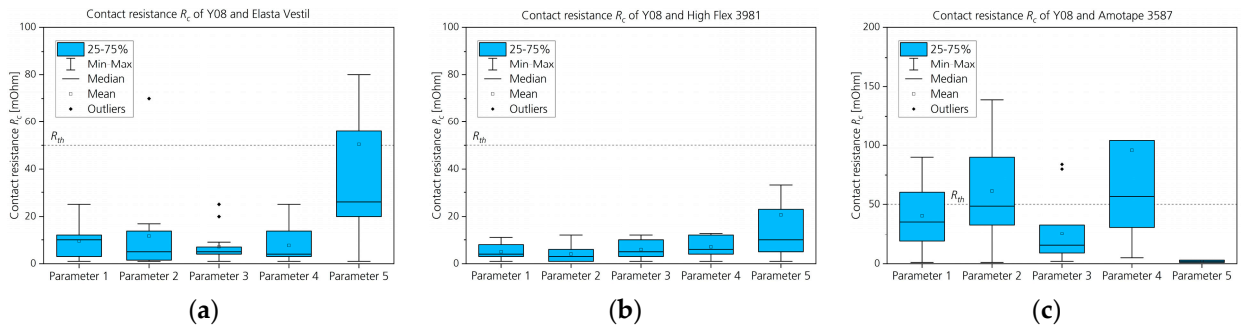


Figure 11. Welded interconnection of hybrid conductive yarn Y08 with three types of conductive ribbons: (a) Elasta Vestil; (b) High Flex 3981; and (c) Amotape 3587.

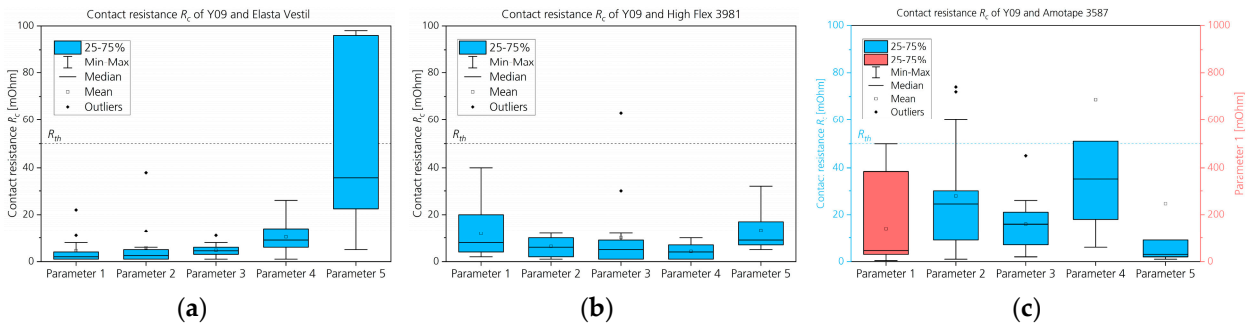


Figure 12. Welded interconnection of hybrid conductive yarn Y09 with three types of conductive ribbons: (a) Elasta Vestil ribbon; (b) High Flex 3981; and (c) Amotape 3587.

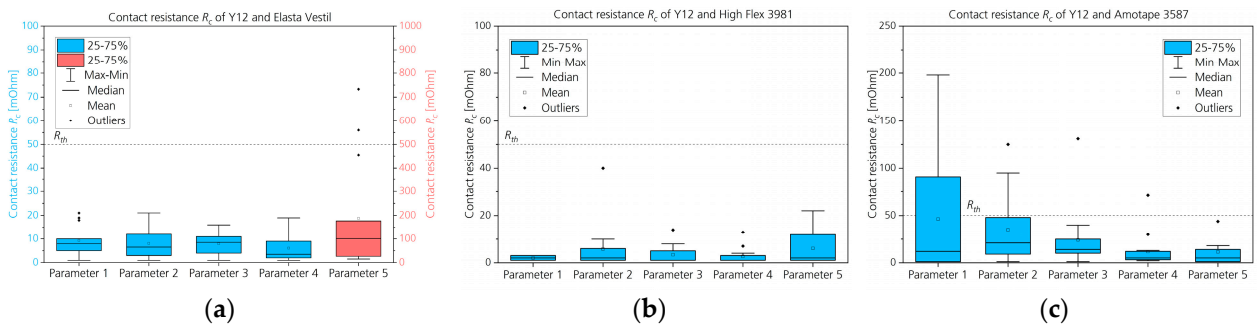


Figure 13. Welded interconnection of hybrid conductive yarn Y12 with three types of conductive ribbons: (a) Elasta Vestil; (b) High Flex 3981; and (c) Amotape 3587.

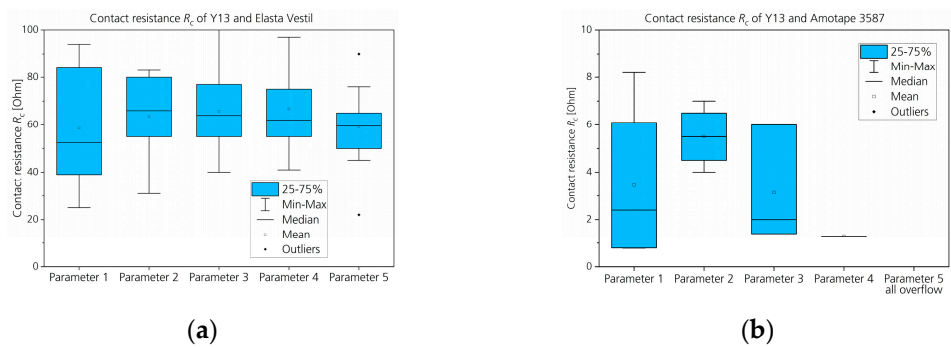


Figure 14. Welded interconnection of hybrid conductive yarn Y13 with two types of conductive ribbons: (a) Elasta Vestil; and (b) Amotape 3587.

Table 6 shows the percentage of contact failures for all results, which indicates the quality of the ultrasonic welding process for each material and parameter, except the high

impedance Y13 contact resistances. A failure indicates a contact resistance over 50 mOhm or no contact measured. Note that, as listed in Table 5, each material combination has different parameters for speed and gap size for numbers 1–5.

Table 6. Failure rate of welded ribbons interconnected with conductive yarns for all parameters.

Conductive Ribbon	Interconnected with	Failure Rate (%) for Parameter 1	Failure Rate (%) for Parameter 2	Failure Rate (%) for Parameter 3	Failure Rate (%) for Parameter 4	Failure Rate (%) for Parameter 5
Elasta Vestil	Y08	14.3	14.3	0	0	42.9
	Y09	0	0	0	7.1	50
	Y12	0	0	0	0	57.1
High Flex 3981	Y08	0	0	0	0	6.7
	Y09	0	0	6.7	0	0
	Y12	0	0	0	0	0
Amotape 3587	Y08	26.7	46.7	13	60	100
	Y09	33.3	20	0	26.7	33.3
	Y12	40	20	6.7	6.7	13.3

In the welding interconnection tests, the Elasta Vestil ribbon performed well as low contact resistances could be determined over a wide window of welding parameters with low failure rates. After TPU embedding, High Flex 3981 not only offered the best adhesion to the textile substrate, but of the three conductive ribbons tested, it achieved the best electrical results, which could be due to the material structure having a large metallic surface contact area and a ductile polymer core. In addition, not only are the contact resistances low, but the process yield is also high over a large parameter window. With Amotape 3587, however, the defect rate is higher with a relatively high contact resistance compared with the other two ribbon variants.

A few optimizations were carried out for the second final batch of test vehicles. First, AMOHR Technische Textilien GmbH developed and provided the new Amotape 46050, which consists of crossing, silver-plated copper strands and thus, like the other ribbons, has an advantageous parallel connection of the individual metal strands resulting in lower conductor resistances. Furthermore, additional hotmelt adhesive yarns were incorporated into the conductive ribbon, which improved the mechanical adhesion to the textile substrate.

The best values from the evaluations of the first batch were selected as final welding parameters and are listed in Table 7. Due to the similar material thicknesses, the welding parameters determined for Amotape 3587 were also used for Amotape 46050. However, to reduce the test matrix and the testing workload, only two yarn variants were used in the final batch, Y08 and Y12.

Table 7. Overview of the determined welding parameters for the final batch.

Conductive Yarn	Interconnected with	Power P (W)	Force F (N)	Speed v (m/min)	Gap Size s (mm)
Y08	Elasta Vestil	100	100	0.4	0.4
	High Flex 3981	100	100	0.2	0.2
	Amotape 46050	100	100	0.2	0.2
Y12	Elasta Vestil	100	100	0.4	0.55
	High Flex 3981	100	100	0.2	0.25
	Amotape 46050	100	100	0.2	0.35

3.3. Results of the Reliability Tests

After ultrasonic welding, the initial contact resistances were measured and then the specimens were tested using the test methods described in Section 2.9. For this purpose, the batch of samples was evenly divided into four parts. After completion of the reliability tests, all contact resistances were again determined by means of a four-point measurement.

The results for the final batch are shown in the following Figures 15–17. For a simplified overview, all the initial contact resistances are listed as mean values. For welding of Y08 with Elasta Vestil, the mean value is 3.75 mOhm, for High Flex 3981 it is 1.0 mOhm and for Amotape 46050 it is 1.1 mOhm. For contacting Y12, the mean values are 5.0 mOhm for Elasta Vestil, 4.25 mOhm for High Flex 3981 and 1.0 mOhm for Amotape 46050.

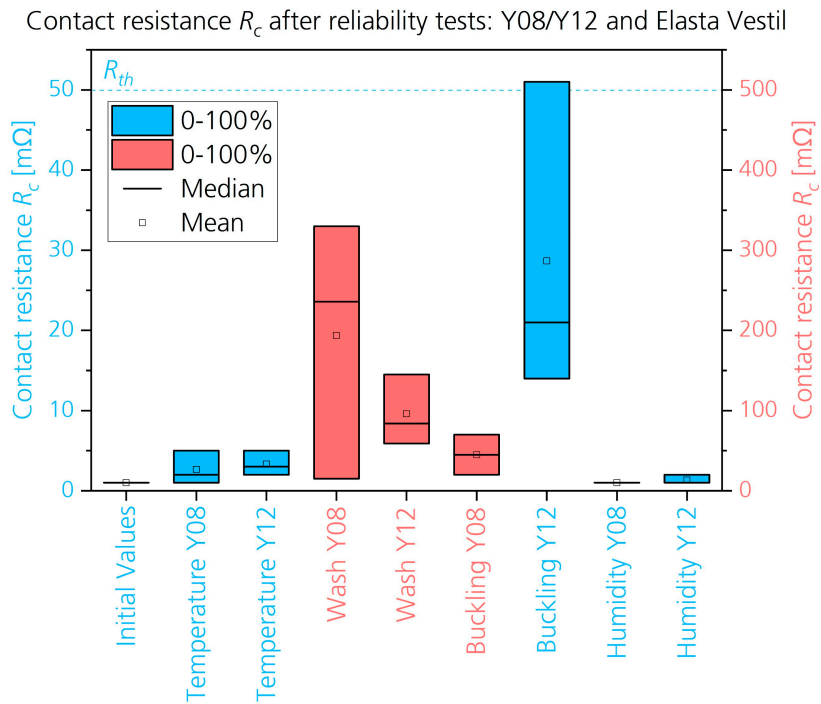


Figure 15. Influence of reliability tests on contact resistance for welding with Elasta Vestil.

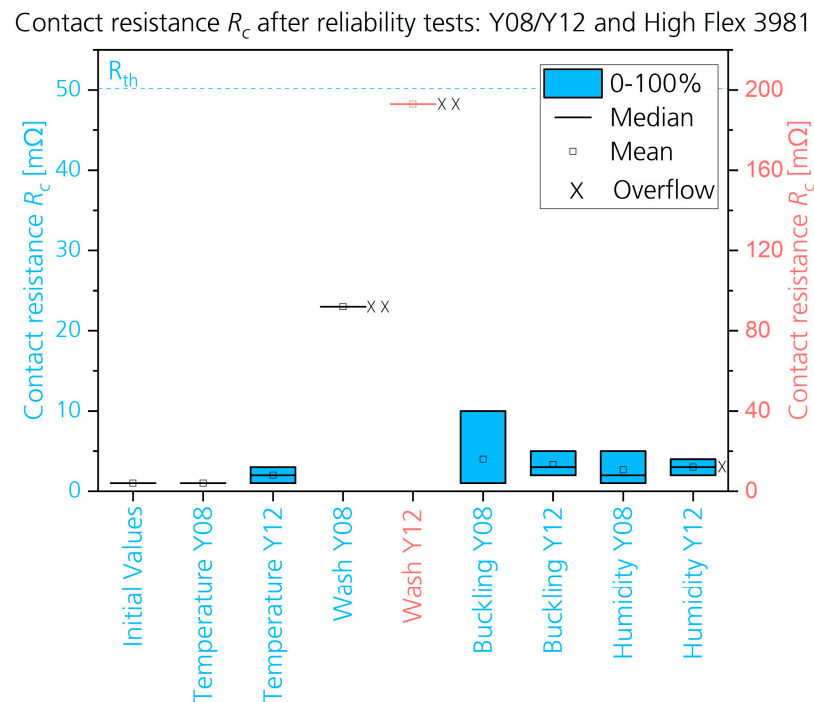


Figure 16. Influence of reliability tests on contact resistance for welding with High Flex 3981.

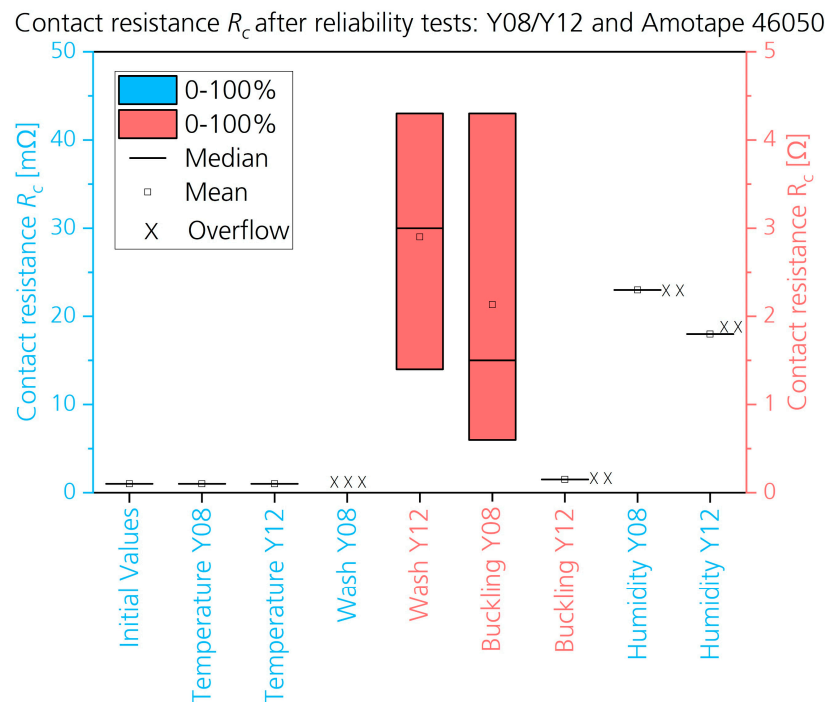


Figure 17. Influence of reliability tests on contact resistance for welding with Amotape 46050.

Based on a five-point rating scale, the individual test results are summarized in Table 8.

Table 8. Evaluation of the influence of the reliability tests on the welded contact resistances.

Reliability Test	Conductive Yarn	Elasta Vestil	High Flex 3981	Amotape 46050
Temperature Cycle	Y08	excellent	excellent	excellent
	Y12	excellent	excellent	excellent
Damp/Heat	Y08	excellent	excellent	good
	Y12	excellent	good	good
Buckling	Y08	fair	excellent	poor
	Y12	good	excellent	bad
Washability	Y08	poor	poor	bad
	Y12	poor	bad	bad

3.4. Optical Analysis of the Electrical Interconnection

To gain an initial insight into the ultrasonically welded contact structures, cross-sections of unstressed specimens were prepared and examined on a Keyence VHX-6000 digital light microscope. Figure 18 shows a cross-section of a contact between the individual conductors of the High Flex 3981 ribbon and Y08 yarn. Material compression and deformation of the metal strands in the contact area and the stamp imprint of the knurled welding wheel on the material surface are clearly visible.

All the samples were further inspected with a Phoenix nanome x 180 X-ray microscope before and after the reliability tests. No conductor breakages that could occur due to the ultrasonic vibrations were detected in any of the samples. An exemplary image of a contacted sample is shown in Figure 19a. Using X-ray microcomputed tomography (μ -CT) with a Phoenix nanotom m 180, selected samples were scanned three-dimensionally to gain a more detailed insight into the contact structure. A μ -CT image is shown in Figure 19b.

3.5. Functional Samples with Continuously Ultrasonic Welded Contacts

Various electrically heatable functional samples were prepared to demonstrate the developed interconnection technology as heatable textiles also account for the largest share of the e-textile market [3] (p. 11). First, textile samples with embroidered or knitted

Y08 heating yarns were produced, and then the integrated yarns were connected with conductive ribbons using US welding. Figures 20 and 21 show two such demonstrators. The flat, flexible structures of the contact tapes, which bond seamlessly to the textile substrate, as well as the low contact resistance, can be seen in the attached (thermal) images. Figure 22 shows the final demonstrator, which consists of a 190 cm × 90 cm large knitted bed sheet with knitted heating conductors made of Y08 yarn, onto which Elasta Vestil ribbons were welded on the upper and lower sides so that all parallel-running heating conductors were electrically and mechanically interconnected.

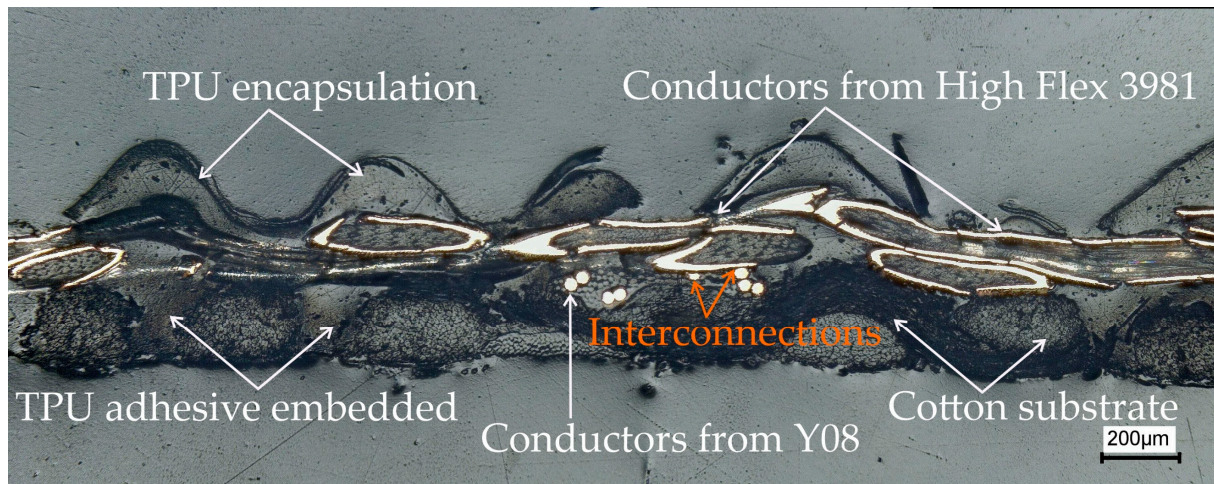
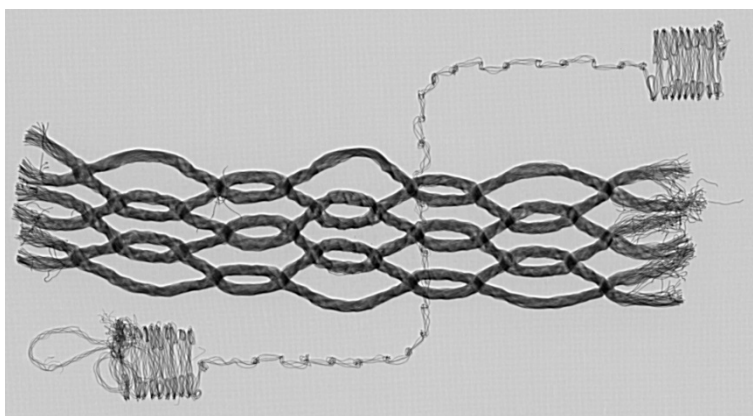


Figure 18. Cross-section of an ultrasonically welded interconnection between High Flex 3981 ribbon and Y08 yarn.



(a)



(b)

Figure 19. Non-destructive optical analysis of the welded interconnections: (a) X-ray image of a welded contact between Amotape 46050 and Y08; and (b) µ-CT scan of a welded contact between Amotape 46050 and Y08.

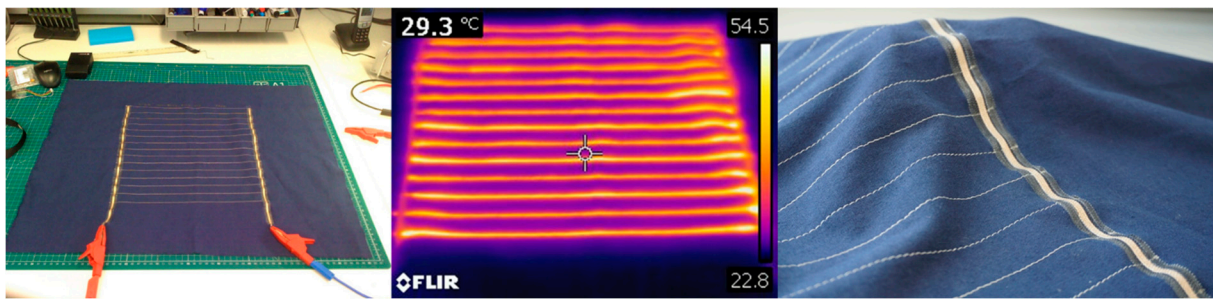


Figure 20. Heatable functional demonstrator made of embroidered Y08 yarn and welded contact ribbon High Flex 3981.

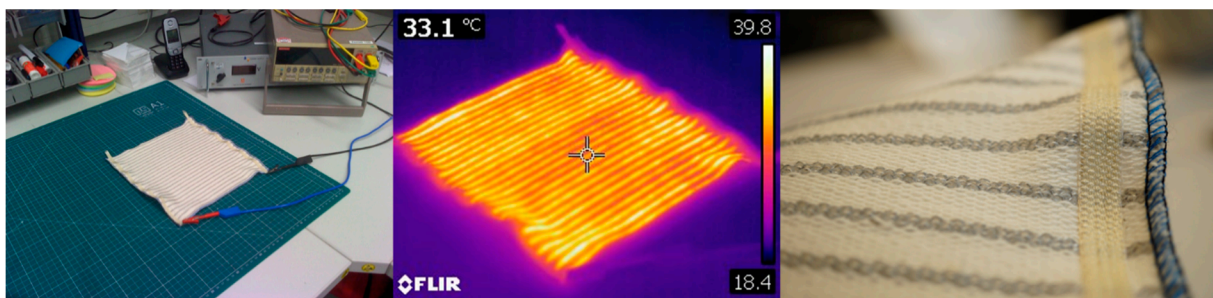


Figure 21. Heatable functional demonstrator made of knitted Y08 yarn and welded contact ribbon Elasta Vestil.



Figure 22. A 90 cm × 190 cm knitted bed sheet with integrated Y08 yarns, ultrasonically welded with conductive ribbon Elasta Vestil as a continuous contact element for the interconnection of the heating yarns.

4. Discussion

A new joining method for continuous electrical interconnections of textile-integrated conductors with conductive ribbons attached by means of rotary ultrasonic plastic welding has been proposed, tested and investigated. For this study, four selected hybrid conductive yarns were embroidered onto a cotton substrate and then woven or braided commercial conductive ribbons were welded onto the yarns by a flatbed ultrasonic welding machine equipped with a knurled steel anvil wheel and sonotrode as welding tools. Thermoplastic films laminated onto the ribbons or hot melt yarns already woven into the ribbons were tested as adhesives for a stable mechanical joint. As the TPU-coated ribbons shrank by 7–8% during ultrasonic welding, the ribbon length had to be individually adjusted for the experiments.

Empirical experiments were used to determine the optimum welding parameters. By measuring the highest peel forces of the welded conductive ribbons on cotton fabric, the welding power P of 100 W, welding force F of 100 N and welding speed v between 0.2 and 0.4 m/min were determined as optimal, and no influence of the conductive ribbon or adhesive on these results was observed. In contrast, the different material thicknesses strongly influenced the welding parameter gap size s . In extensive tests, the optimal gap sizes could be determined for each material combination by means of a four-point resistance measurement of the contact resistances achieved. Thus, a continuous ultrasonic welding process setup could be determined for each material combination, with the best results having a 100% yield and low contact resistances in the range of 1 - 10 mOhm.

In evaluating the reliability tests, washability remains the biggest challenge for e-textiles, whereas the ultrasonically welded contacts showed no or only minor ageing or failure after the climatic and mechanical tests. Some samples showed delamination between the textile substrate and conductive ribbon during the buckling or washing test, mainly with Elasta Vestil and Amotape 46050, which also had significantly lower peel forces than High Flex 3981. In the case of High Flex 3981, the TPU top layer was damaged during washing, causing the then no longer encapsulated conductive ribbon to twist and so partially loosen from the textile structure during the washing cycles.

The X-ray analysis did not show any broken conductors, but in the μ -CT images, several conductor fractures could be identified where the metal wires from the ribbons came into contact with those from the hybrid conductive yarns. This indicates that the brittle metal wires could break in some cases during ultrasonic welding. However, due to the redundant design with numerous conductors running in parallel for the conductive ribbons and yarns, this did not result in contact failure. The broken conductors as well as all the conductive materials are embedded so well in the textile and thermoplastic matrix that even extreme loads such as the buckling test did not lead to contact failure.

5. Conclusions

This study has proven that the continuous ultrasonic welding technique is suitable for the manufacturing of multiple interconnects for large-area e-textiles. Although washability has not yet been achieved, we see the greatest advantage in realizing a flat, flexible as well as thermally and mechanically stable interconnection and thus realizing a reliable contact between hybrid conductive yarns and potentially endless conductive ribbons. The reparability option and possible separation of the conductive ribbons in a recycling process at the end of the life cycle—due to thermoplastic adhesives, which can be softened again and thus detached from the textile substrate—also adds to the sustainability of the interconnection method.

The use of commercial materials as well as an established textile manufacturing technique enables a fast technology transfer into industry. The first areas of application for continuous ultrasonic welding could be in the production of large-area heating textiles, for example as seat heating in cars, as indoor wall heaters, and also for cut-detection sensor fabrics in truck tarpaulins or house roofs.

In the future, further development of the conductive ribbons could achieve higher reliability and thus open up new fields of application, for example, in smart clothing. For this purpose, investigations into suitable thermoplastics are planned, in particular, the use of different and thicker TPU films for better encapsulation of the metallic conductors, tests with low-melting films to increase the process speed and tests to increase adhesion through the integration of suitable TPU-based yarns into the welding area of the textile carrier.

Author Contributions: Conceptualization, methodology, writing—original draft preparation, project administration, funding acquisition, C.D.; investigation, visualization, S.H. and C.D.; writing—review and editing, S.H. and M.S.-R.; supervision, M.S.-R. All authors have read and agreed to the published version of the manuscript.

Funding: The IGF research project (278 EN) of the research association Forschungskuratorium Textil e.V., Reinhardtstraße 14-16, 10117 Berlin was funded via the AiF within the program for supporting the “Industrial Collective Research” (IGF) from funds of the Federal Ministry of Economic Affairs and Climate Actions (BMWK) on the basis of a decision by the German Bundestag.

Institutional Review Board Statement: Not applicable.

Informed Consent Statement: Not applicable.

Data Availability Statement: The data presented in this study are available on request from the corresponding author.

Acknowledgments: The authors would like to thank VÚB a.s. and the RICE research center of the Faculty of Electrical Engineering at the University of West Bohemia for providing test samples with embroidered or knitted hybrid conductive yarns. We would also like to thank the company AMOHR Technische Textilien GmbH for the development and provision of the Amotape 46050, which was carried out after joint discussions within the framework of this study. Further thanks go to our colleagues Lukas Werft for performing the buckling tests and Sigrid Rotzler for proofreading this manuscript.

Conflicts of Interest: The authors declared no potential conflicts of interest with respect to the research, authorship and/or publication of this article. The funders had no role in the design of the study; in the collection, analyses, or interpretation of data; in the writing of the manuscript; or in the decision to publish the results.

References

1. Hughes-Riley, T.; Dias, T.; Cork, C. A Historical Review of the Development of Electronic Textiles. *Fibers* **2018**, *6*, 34. [CrossRef]
2. Fernández-Caramés, T.M.; Fraga-Lamas, P. Towards The Internet of Smart Clothing: A Review on IoT Wearables and Garments for Creating Intelligent Connected E-Textiles. *Electronics* **2018**, *7*, 405. [CrossRef]
3. Hayward, J. *E-Textiles & Smart Clothing 2021–2031: Technologies, Markets and Players*; IDTechEx Reports: Cambridge, UK, 2021.
4. Koncar, V. (Ed.) *Smart Textiles and Their Applications*; Woodhead Publishing: Sawston, UK; Cambridge, UK, 2016.
5. Wicaksono, I.; Cherston, J.; Paradiso, J.A. Electronic Textile Gaia: Ubiquitous Computational Substrates Across Geometric Scales. *IEEE Pervasive Comput.* **2021**, *20*, 18–29. [CrossRef]
6. Repon, M.R.; Mikučionienė, D. Progress in Flexible Electronic Textile for Heating Application: A Critical Review. *Materials* **2021**, *14*, 6540. [CrossRef]
7. Almohammed, B.; Ismail, A.; Sali, A. Electro-textile wearable antennas in wireless body area networks: Materials, antenna design, manufacturing techniques, and human body consideration—A review. *Text. Res. J.* **2021**, *91*, 646–663. [CrossRef]
8. Shi, X.; Zuo, Y.; Zhai, P.; Shen, J.; Yang, Y.; Gao, Z.; Liao, M.; Wu, J.; Wang, J.; Xu, X.; et al. Large-area display textiles integrated with functional systems. *Nature* **2021**, *591*, 240–245. [CrossRef]
9. Chen, G.; Xiao, X.; Zhao, X.; Tat, T.; Bick, M.; Chen, J. Electronic Textiles for Wearable Point-of-Care Systems. *Chem. Rev.* **2022**, *122*, 3259–3291. [CrossRef] [PubMed]
10. Vieira, D.; Carvalho, H.; Providência, B. E-Textiles for Sports: A Systematic Review. *JBBBE* **2022**, *57*, 37–46. [CrossRef]
11. Koncar, V. Smart Textiles for Monitoring and Measurement Applications. In *Smart Textiles for In Situ Monitoring of Composites*; Koncar, V., Ed.; Woodhead Publishing: Duxford, UK, 2019; pp. 1–151.
12. Stanley, J.; Hunt, J.A.; Kunovski, P.; Wei, Y. A review of connectors and joining technologies for electronic textiles. *Eng. Rep.* **2022**, *4*, e12491. [CrossRef]
13. Gehrke, I.; Tenner, V.; Lutz, V.; Schmelzeisen, D.; Gries, T. *Smart Textiles Production: Overview of Materials, Sensor and Production Technologies for Industrial Smart Textiles*; MDPI: Basel, Switzerland, 2019.
14. Rotzler, S.; Kallmayer, C.; Dils, C.; von Krshiwoblozki, M.; Bauer, U.; Schneider-Ramelow, M. Improving the washability of smart textiles: Influence of different washing conditions on textile integrated conductor tracks. *J. Text. Inst.* **2020**, *111*, 1766–1777. [CrossRef]
15. Eppinger, E.; Slomkowski, A.; Behrendt, T.; Rotzler, S.; Marwede, M. Design for Recycling of E-Textiles: Current Issues of Recycling of Products Combining Electronics and Textiles and Implications for a Circular Design Approach. In *Recycling—Recent Advances*; Saleh, H.M., Hassan, A.I., Eds.; IntechOpen: London, UK, 2022; Available online: <https://www.intechopen.com/online-first/84034> (accessed on 22 December 2022). [CrossRef]
16. Simegnaw, A.A.; Malengier, B.; Rotich, G.; Tadesse, M.G.; Van Langenhove, L. Review on the Integration of Microelectronics for E-Textile. *Materials* **2021**, *14*, 5113. [CrossRef]
17. Hoerr, M. Reliable Mass Production of E-Textiles by using Embroidery Technology. Presented at IPC E-Textiles, San Diego, CA, USA, 23 January 2023.
18. Garbacz, K.; Stagon, L.; Rotzler, S.; Semeneč, M.; von Krshiwoblozki, M. Modular E-Textile Toolkit for Prototyping and Manufacturing. *Proceedings* **2021**, *68*, 5. [CrossRef]

19. Linz, T.; von Krshiwoblozki, M.; Walter, H.; Foerster, P. Contacting electronics to fabric circuits with nonconductive adhesive bonding. *J. Text. Inst.* **2012**, *103*, 1139–1150. [CrossRef]
20. Benouakta, S.; Hutu, F.D.; Duroc, Y. Stretchable Textile Yarn Based on UHF RFID Helical Tag. *Textiles* **2021**, *1*, 547–557. [CrossRef]
21. Seyedin, S.; Carey, T.; Arbab, A.; Eskandarian, L.; Bohm, S.; Kim, J.M.; Torrisi, F. Fibre electronics: Towards scaled-up manufacturing of integrated e-textile systems. *Nanoscale* **2021**, *13*, 12818–12847. [CrossRef]
22. Dhawan, A.; Seyam, A.M.; Ghosh, T.K.; Muth, J.F. Woven fabric-based electrical circuits: Part I: Evaluating interconnect methods. *Text. Res. J.* **2004**, *74*, 913–919. [CrossRef]
23. Zhang, H. Flexible textile-based strain sensor induced by contacts. *Meas. Sci. Technol.* **2015**, *26*, 105102. [CrossRef]
24. Suchý, S.; Kalaš, D.; Kalčík, J.; Soukup, R. A comparison of resistance spot and ultrasonic welding of hybrid conductive threads. In Proceedings of the 43rd International Spring Seminar on Electronics Technology (ISSE), Demanovska Valley, Slovakia, 14–15 May 2020; pp. 1–5. [CrossRef]
25. Suchý, S.; Rostás, K.; Soukup, R. Encapsulation Methods for Resistance-Welded Contacts in Smart Textiles. In Proceedings of the 45th International Spring Seminar on Electronics Technology (ISSE), Vienna, Austria, 11–15 May 2022; pp. 1–5. [CrossRef]
26. Locher, I. Technologies for System-on-Textile Integration. Doctoral Thesis, ETH, Zürich, Switzerland, 2006. [CrossRef]
27. Slade, J.R.; Winterhalter, C. Electro-textile garments for power and data distribution. In Proceedings of the Display Technologies and Applications for Defense, Security, and Avionics IX; and Head- and Helmet-Mounted Displays XX (SPIE Defense + Security), Baltimore, MD, USA, 21 May 2015. [CrossRef]
28. Thurner, F. New methods for reliable contacts of conductive textile substrates. *Tech. Text.* **2019**, *62*, 296–298.
29. Micus, S.; Rostami, S.G.; Haupt, M.; Gresser, G.T.; Meghraz, M.A.; Eskandarian, L. Integrating Electronics to Textiles by Ultrasonic Welding for Cable-Driven Applications for Smart Textiles. *Materials* **2021**, *14*, 5735. [CrossRef]
30. Dils, C.; Kallmayer, C.; Gerhold, L.; Schneider-Ramelow, M. Investigations into ultrasonic plastic welding as an innovative contacting technology for the integration of electronics into textiles. *Join. Plast.* **2020**, *14*, 104–110.
31. Dils, C.; Kalas, D.; Reboun, J.; Suchy, S.; Soukup, R.; Moravcova, D.; von Krshiwoblozki, M.; Schneider-Ramelow, M. Interconnecting embroidered hybrid conductive yarns by ultrasonic plastic welding for e-textiles. *Text. Res. J.* **2022**, *92*, 4501–4520. [CrossRef]
32. Atalay, O.; Kalaoglu, F.; Bahadir, S.K. Development of textile-based transmission lines using conductive yarns and ultrasonic welding technology for e-textile applications. *J. Eng. Fibers Fabr.* **2019**, *14*, 1–8. [CrossRef]
33. Leśnikowski, J. Research into the Textile-Based Signal Lines Made Using Ultrasonic Welding Technology. *Autex Res. J.* **2022**, *22*, 11–17. [CrossRef]
34. Platilon TPU Films. Available online: <https://solutions.covestro.com/en/brands/platilon> (accessed on 30 November 2022).
35. Löher, T.; Seckel, M.; Ostmann, A. Stretchable electronics manufacturing and application. In Proceedings of the 3rd Electronics System Integration Technology Conference (ESTC), Berlin, Germany, 13–16 September 2010; pp. 1–6. [CrossRef]
36. Zoschke, K.; Löher, T.; Kallmayer, C.; Jung, E. Flexible and Stretchable Systems for Healthcare and Mobility. In *Flexible, Wearable, and Stretchable Electronics*, 1st ed.; Katsuyuki, S., Ed.; CRC Press: Boca Raton, FL, USA, 2020; pp. 269–282.
37. Dils, C.; Werft, L.; Walter, H.; Zwanzig, M.; von Krshiwoblozki, M.; Schneider-Ramelow, M. Investigation of the Mechanical and Electrical Properties of Elastic Textile/Polymer Composites for Stretchable Electronics at Quasi-Static or Cyclic Mechanical Loads. *Materials* **2019**, *12*, 3599. [CrossRef]
38. von Krshiwoblozki, M.; Linz, T.; Neudeck, A.; Kallmayer, C. Electronics in Textiles—Adhesive Bonding Technology for Reliably Embedding Electronic Modules into Textile Circuits. *Adv. Sci. Technol.* **2012**, *85*, 1–10. [CrossRef]
39. *IPC-TM-650 TEST METHODS MANUAL no. 2.4.9: Peel Strength, Flexible Printed Wiring Materials*; The Institute for Interconnecting and Packaging Electronic Circuits: Northbrook, IL, USA, 1988.
40. *EN 16812:2016; Textiles and Textile Products—Electrically Conductive Textiles—Determination of the Linear Electrical Resistance of Conductive Tracks; German Version*. European Committee for Standardization: Brussels, Belgium, 2016.
41. Agcayazi, T.; Chatterjee, K.; Bozkurt, A.; Ghosh, T.K. Flexible Interconnects for Electronic Textiles. *Adv. Mater. Technol.* **2018**, *3*, 1700277. [CrossRef]
42. Biermaier, C.; Bechtold, T.; Pham, T. Towards the Functional Ageing of Electrically Conductive and Sensing Textiles: A Review. *Sensors* **2021**, *21*, 5944. [CrossRef]
43. Persons, A.K.; Ball, J.E.; Freeman, C.; Macias, D.M.; Simpson, C.L.; Smith, B.K.; Burch V., R.F. Fatigue Testing of Wearable Sensing Technologies: Issues and Opportunities. *Materials* **2021**, *14*, 4070. [CrossRef]
44. Decaens, J.; Vermeersch, O. Specific testing for smart textiles. In *Advanced Characterization and Testing of Textiles*, 1st ed.; Dolez, P., Vermeersch, O., Izquierdo, V., Eds.; Elsevier: Cambridge, UK, 2018; pp. 351–374. [CrossRef]
45. Shuvo, I.I.; Decaens, J.; Lachapelle, D.; Dolez, P.I. Smart textiles testing: A roadmap to standardized test methods for safety and quality-control. In *Textiles for Functional Applications*, 1st ed.; Kumar, B., Ed.; IntechOpen: London, UK, 2021; pp. 1–15. Available online: <https://www.intechopen.com/chapters/75712> (accessed on 22 December 2022). [CrossRef]
46. *IEC 60068-2-14:2009; Environmental Testing—Part 2-14: Tests—Test N: Change of Temperature; German Version*. International Electrotechnical Commission: Geneva, Switzerland, 2009.
47. *IEC 60068-2-1:2007; Environmental Testing—Part 2-1: Tests—Test A: Cold; German Version*. International Electrotechnical Commission: Geneva, Switzerland, 2007.

48. IEC 60068-2-78:2012; Environmental Testing—Part 2-78: Tests—Test Cab: Damp Heat, Steady State; German Version. International Electrotechnical Commission: Geneva, Switzerland, 2013.
49. Rotzler, S.; von Krshiwoblozki, M.; Schneider-Ramelow, M. Washability of e-textiles: Current testing practices and the need for standardization. *Text. Res. J.* **2021**, *91*, 2401–2417. [[CrossRef](#)]
50. Rotzler, S.; Schneider-Ramelow, M. Washability of E-Textiles: Failure Modes and Influences on Washing Reliability. *Textiles* **2021**, *1*, 37–54. [[CrossRef](#)]
51. Rotzler, S.; Schneider-Ramelow, M. Development of a Testing Protocol to Assess the Washability of E-Textiles. *Solid State Phenom.* **2022**, *333*, 3–10. [[CrossRef](#)]

Disclaimer/Publisher’s Note: The statements, opinions and data contained in all publications are solely those of the individual author(s) and contributor(s) and not of MDPI and/or the editor(s). MDPI and/or the editor(s) disclaim responsibility for any injury to people or property resulting from any ideas, methods, instructions or products referred to in the content.